Neural Network-based Single-material Beam Hardening Correction for X-ray CT in Additive Manufacturing

Obaidullah Rahman[1], Singanallur V. Venkatakrishnan[1], Zackary Snow[1], Paul Brackman[2], Thomas Feldhausen[1], Ryan Dehoff[1], Vincent Paquit[1], and Amirkoushyar Ziabari[1]

[1]Oak Ridge National Lab (ORNL), Oak Ridge, TN 37830, USA
[2]Carl Zeiss Industrial Metrology, LLC, Maple Grove, MN 55369, USA

Abstract Beam-hardening (BH) artifacts are ubiquitous in X-ray CT scans of additively manufactured (AM) metal components. While linearization approaches are useful for correcting beam-hardened data from single material objects, they either require a calibration scan or detailed system and material composition information. In this paper, we introduce a neural network-based, material-agnostic method to correct beam-hardening artifacts. We train a neural network to map the acquired beam-hardened projection values and the corresponding estimated thickness of the object based on an initial segmentation to beam-hardening related parameters, which can be used to compute the coefficients of a linearizing correction polynomial. A key strength of our approach is that, once the network is trained, it can be used for correcting beam hardening from a variety of materials without any calibration scans or detailed system and material composition information. Furthermore, our method is robust to errors in the estimated thickness due to the typical challenge of obtaining an accurate initial segmentation from reconstructions impacted by BH artifacts. We demonstrate the utility of our method to obtain high-quality CT reconstructions from a collection of AM components – suppressing cupping and streaking artifacts.

1 Introduction

X-ray CT reconstruction of AM components provides insight on defects [1, 2] introduced by the manufacturing process, allowing manufacturers to understand the impact of process parameters on part performance and, in turn, design consistent and reliable components. However, the complex attenuation of poly-chromatic X-rays as they propagate through dense metals results in beam-hardening (BH) artifacts, such as cupping and streaks, which make it challenging to detect microstructurally relevant features (e.g., cracks, porosity) in typical reconstructions. Methods to address BH can be broadly classified into hardware and algorithmic approaches [3, 4]. Hardware approaches involve filtering the X-ray beam to suppress higher energies, but this method reduces the flux, leading to poor reconstruction quality when the measurement times are kept the same. This method also requires an expert user to select the appropriate filter depending on the sample to be scanned. In contrast, software approaches include the use of a heuristic polynomial to linearize the normalized data [5] prior to the reconstruction, and more computationally expensive methods that attempt to model the non-linearities of the image formation process [6].

For industrial X-ray CT systems, linearization approaches are preferred due to their low computational complexity. These methods involve applying a polynomial correction to the normalized measurement data so that the projection vs thickness curve (p vs d) for the material is a straight line instead of the typical curve seen particularly at higher thickness values. In order to obtain this p vs d curve, one has to manufacture and measure a calibration wedge sample [3] corresponding to the same material as the component to be measured. For single material components, the linearization polynomial can be computed in theory even without a calibration sample, but this requires knowledge of source spectrum, filtering hardware specifications, and detailed knowledge of the detector spectral response to obtain the p vs d curve which is often impractical.

In this paper, we propose a new linearization approach based on the use of a neural network (NN). We first train a NN to map between the projected value and corresponding thickness to the parameters of a Van de Casteel attenuation model [7] by synthetically generating several test (p, d) data points. During inference time, the thickness values corresponding to each measurement are obtained by projecting an initial binary segmentation of the reconstruction obtained using the FDK algorithm [8]. Thus, we effectively obtain the parameters of a Van de Casteel model from the neural network, which can then be used to compute the linearization polynomial. The main advantage of our method is that it once it is trained for a collection of (p, d) data points, it can be used to correct for BH due to a range of materials. We demonstrate the value of our method by suppressing BH artifacts for numerous AM components made of different materials without any manual tuning of the algorithm - enabling a fully automated workflow for X-ray CT of metal AM components that produces high quality reconstructions. Furthermore, our method is robust against imperfect p vs d values due to an imprecise segmentation - a common occurrence for dense parts with complex geometries.

2 Method

Our method to correct for BH from single material scans consists of three steps: 1) use a NN to map *each* projection and estimated thickness value to the parameters of a BH

Corresponding author's email address: *rahmano@ornl.gov*. Research sponsored by the US Department of Energy, Office of Energy Efficiency and Renewable Energy, Advanced Manufacturing Office and Technology Commercialization Fund (TCF-21-24881), under contract DE-AC05-00OR22725 with UT-Battelle, LLC. The US government retains and the publisher, by accepting the article for publication, acknowledges that the US government retains a nonexclusive, paid-up, irrevocable, worldwide license to publish or reproduce the published form of this manuscript, or allow others to do so, for US government purposes. DOE will provide public access to these results of federally sponsored research in accordance with the DOE Public Access Plan (http://energy.gov/downloads/doe-public-access-plan).

model, 2) average the model parameters estimated by the NN for all the (p,d) values and 3) use the averaged model parameters to compute an 8^{th} order linearization polynomial. We train the proposed network solely on synthetically generated data using the bimodal energy model for BH from [7]. It was demonstrated in [7] that BH can be simplified using two dominant X-ray energies, E_1 and E_2, where μ_1 and μ_2 are the corresponding linear attenuation coefficients (LAC) of the material. The material's non-linear projection vs thickness can be obtained using

$$p_{bh} = \mu_2 d + \ln \frac{1+\alpha}{1+\alpha e^{-(\mu_1-\mu_2)d}} \tag{1}$$

where the left hand side is the BH-affected projection, α represents the ratio of the source-detector efficiency at said x-ray energies, and d is the distance the x-ray beam has to traverse within the material. The ideal (BH-free) projection, which varies linearly with distance, is given by

$$p_{bhc} = \frac{\alpha\mu_1 + \mu_2}{1+\alpha} d \tag{2}$$

2.1 Training

We used a NN, consisting of 16 fully connected layers with 512 neurons with biases and a ReLU activation, which we call beam-hardening correction network (BHCN). The input layer consists of 2 nodes for the projection value and associated thickness and the output layer consists of 3 nodes for the parameters of the model in (1). To get training data, we randomly generate vectors of d^{tr}, α^{tr}, μ_1^{tr}, and μ_2^{tr}, each uniformly drawn from its realistic range.

$$\begin{aligned}
d_i^{tr} &\sim U(0\ mm,\ 20\ mm)\\
\alpha_i^{tr} &\sim U(4,\ 8)\\
\mu_{1,i}^{tr} &\sim U(0.3\ mm^{-1},\ 0.6\ mm^{-1})\\
\mu_{2,i}^{tr} &\sim U(0.03\ mm^{-1},\ 0.15\ mm^{-1})\\
p_i^{tr} &= \mu_{2,i}^{tr} d_i^{tr} + \ln \frac{1+\alpha_i^{tr}}{1+\alpha_i^{tr}\exp\{-(\mu_{1,i}^{tr}-\mu_{2,i}^{tr})d_i^{tr}\}}
\end{aligned}$$

Our claim is that the network will not need to know the material and should be able to estimate BHC parameters only from projection and distance data. Therefore we feed BHCN the pair (p^{tr}, d^{tr}) as input and train it by minimizing the weighted mean absolute error,

$$\frac{1}{N}\sum_{i=1}^{N} |\alpha_i^{tr} - \alpha_i^{out}| + 2|\mu_{1,i}^{tr} - \mu_{1,i}^{out}| + 5|\mu_{2,i}^{tr} - \mu_{2,i}^{out}|$$

The weight were empirically chosen so the losses from individual parameters are somewhat comparable, and one does not overwhelm the other.

2.2 Inference

In order to obtain parameters of the Van de Casteel model from the BHCN, we first reconstruct the measured data using the FDK algorithm. Next, we obtain a binary segmentation of this reconstruction using Otsu's algorithm [9] and forward project it to obtain the distance traversed corresponding to each measured projection. Then, BH-affected projection and distance vectors are fed into the BHCN to get estimates of vectors α, μ_1 and μ_2. For each input data point the BHCN outputs a set of parameters. Since the input is "noisy" because of the erroneous segmentation, the output (BHC parameters) is expected to be "noisy" too. Taking respective means of the output vector estimates yields a "noise-free"/reliable version of the BHC parameters. Then, BH correction in projection using those parameters is followed by FDK reconstruction. The overall inference is outlined in Algorithm 1.

Algorithm 1: BHCN inference

$d_{max} \leftarrow$ largest expected object thickness;
$\varepsilon_d \leftarrow$ distance step size for polynomial fit, $n \leftarrow 8$;
$p \leftarrow$ BH-affected projection, $Im_{BH} \leftarrow FDK(p)$;
$Im_{BH}[\text{metal}] \leftarrow 1$, $Im_{BH}[\text{background}] \leftarrow 0$;
$d \leftarrow$ Forward project(Im_{BH});
for *each i* **do**
  $[\alpha_i^{est}, \mu_{1,i}^{est}, \mu_{2,i}^{est}] \leftarrow BHCN([p_i, d_i])$;
end
$\alpha \leftarrow \frac{1}{N}\sum_{i=1}^{N}\alpha_i^{est}$, $\mu_1 \leftarrow \frac{1}{N}\sum_{i=1}^{N}\mu_{1,i}^{est}$, $\mu_2 \leftarrow \frac{1}{N}\sum_{i=1}^{N}\mu_{2,i}^{est}$;
$d_{vec} \leftarrow [0,\ \varepsilon_d,\ 2\varepsilon_d, \ldots, d_{max}]$;
$proj_{bh} \leftarrow \mu_2 d_{vec} + \ln\frac{1+\alpha}{1+\alpha e^{-(\mu_1-\mu_2)d_{vec}}}$;
$proj_{bhc} \leftarrow \frac{\alpha\mu_1+\mu_2}{1+\alpha} d_{vec}$;
$f_{polyfit} \leftarrow$ poly. fit$(proj_{bh}, proj_{bhc}, n, d_{vec})$;
$p_{correct} \leftarrow f_{polyfit}(p)$, $Im_{BHC} \leftarrow FDK(p_{correct})$;

3 Results

In Sec. 3.1, we compare our method with a baseline curve-fit method and demonstrate that the baseline method can fail in practical conditions. In Sec. 3.2, we compare our method to a more robust, CAD- and physics–based, method.

3.1 Comparison with a curve-fit (trivial BHC) method

One method to estimate BH model parameters from BH-affected projections is by minimizing the difference between the model, i.e. Eq. (1), and the actual projection i.e. simple curve fitting (CF) using

$$(\alpha^{CF}, \mu_1^{CF}, \mu_2^{CF}) = \underset{\alpha^{CF},\mu_1^{CF},\mu_2^{CF}}{\operatorname{argmin}} \{| p - p_{model} |_2\} \tag{3}$$

where p_{model} is computed from Eq. (1) using the distance and current iteration $(\alpha^{CF}, \mu_1^{CF}, \mu_2^{CF})$.

3.1.1 Simulation data

We start with simulation data to compare the BHCN and the curve-fit methods by creating a synthetic metal component with BH parameters $(\alpha^{GT}, \mu_1^{GT}, \mu_2^{GT})$). Forward-projecting the metal mask provides d^{GT}, which, together with the BH parameters, is used to obtain p_{bh} using Eq. (1) and p_{bhc} using Eq. (2). We feed the vector pair (p_{bh}, d) to BHCN and curve-fit methods. The estimated $(\alpha^{BHCN}, \mu_1^{BHCN}, \mu_2^{BHCN})$ and $(\alpha^{CF}, \mu_1^{CF}, \mu_2^{CF})$ will be used to get the BHC projections

p_{BHCN} and p_{CF}, respectively. In the first case, which is ideal, d is exactly known, i.e. $d = d^{GT}$. This corresponds to the top left subfigure in Fig. 1. The rest of the subfigures, in clockwise direction, correspond to increasingly erroneous d supplied to the two competing algorithms. d is the result of incorrect segmentation (either metal declared as background, or background declared as metal) of the uncorrected FDK reconstruction using different threshold values for each of the 5 remaining scenarios. Such challenges are common when segmenting XCT scans of dense metal components with complex shapes.

It can be seen that in the ideal case, they both perform quite well, and the BHC projection vs distance from both algorithms coincide with the ground truth projection. As the segmentation starts to deteriorate, the curve-fit algorithm performance degrades more than BHCN, as seen in the departure of its curve from that of GT. After analysing the p vs d

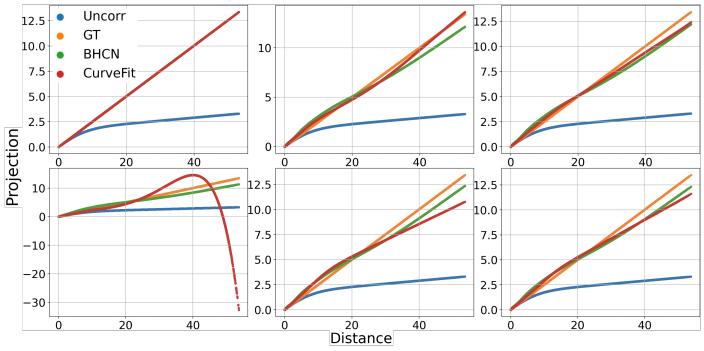

Figure 1: p vs d curve for increasingly worsening segmentation starting with top left in clockwise direction. Curve-fit degrades more than BHCN as segmentation becomes more inaccurate.

curves, we perform FDK reconstruction for each method and for each segmentation case. Fig. 2 corresponds to the reconstructions from the bottom left scenario from Fig. 1. This is the worst segmentation case among the six. The three slices shown demonstrate the robustness of BHCN over CF in case of incorrect segmentation, a common issue with complex component geometry, scattering, noise, etc.

3.1.2 Experimental data

Fig. 3 demonstrates the performance of BHCN and curve-fit algorithms on an experimental data set - a scan of a steel turbine blade. Due to severe beam hardening, the binary segmentation has large errors. We observe that the proposed BHCN helps suppress cupping artifacts compared to the uncorrected image, while CF has made beam hardening worse and introduced artifacts.

3.2 Comparison with CAD- and physics–based BHC method

The CAD- and physics–based model proposed in [10, 11] was used to estimate the BHC parameters for alloys in our case studies and to generate a baseline reference to compare BHCN against. We refer to this method for BH artifact reduction as *reference*. When new alloys are developed, the elemental composition also changes, so the reference model would require re-estimation of the beam-hardening

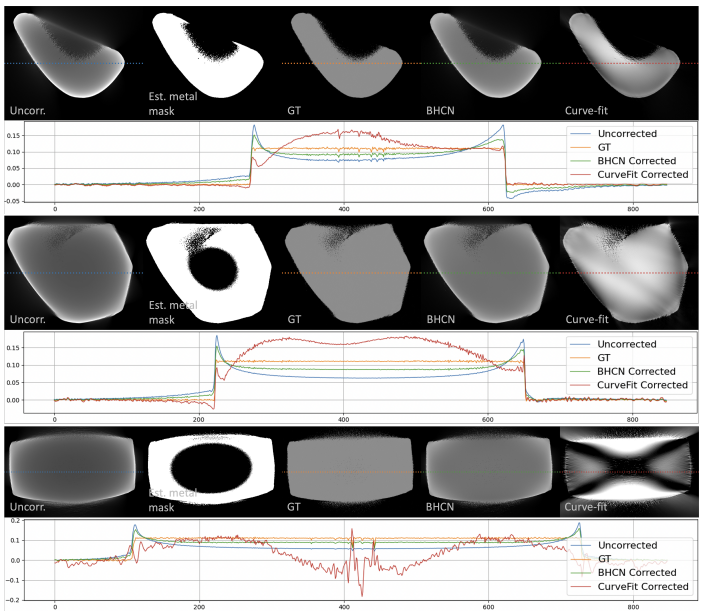

Figure 2: Example of incorrect segmentation of uncorrected FDK from simulated data from Fig. 1 bottom left p vs d curve. The top row of the 3 subfigures indicate different slices of the reconstruction image. (left to right): Uncorrected FDK, incorrect metal mask, ground truth, BHCN, CF. Bottom row of the subfigures: Profile plots. Curve-fit has introduced artifacts and incorrect intensities, and its profile plot, compared to BHCN's, deviates more from that of GT.

parameters. However, our universal BHC method is robust for different alloys without any need for re-calibration.

3.2.1 Robustness across materials

To compare BHCN images with reference images, AM components with complex geometries, including cylinders, poles, fins, and inclines, were constructed from aluminium-cerium (AlCe), stainless steel (316L), and nickel-cobalt (NiCo). In Fig. 4, the reconstruction without any BHC, displays a high degree of beam hardening. Both BHCN and the reference method have similar reduction in BH, as highlighted by the profile plots. The inset shows an expanded view of the ROI marked in each image, highlighting the better contrast of the BH corrected images near flaws in both BH corrected images.

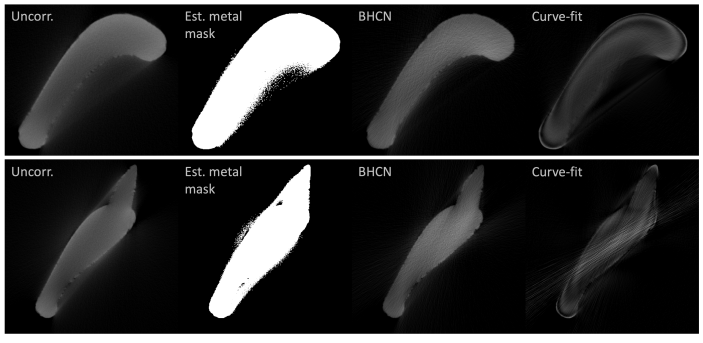

Figure 3: 2 slices from the reconstruction of a real turbine blade scan (left to right) Uncorrected, estimated metal mask, BHCN corrected, curve-fit corrected. BHCN makes the metal component of the image more uniform, but curve-fit seems to introduce strange intensities and distort the shape.

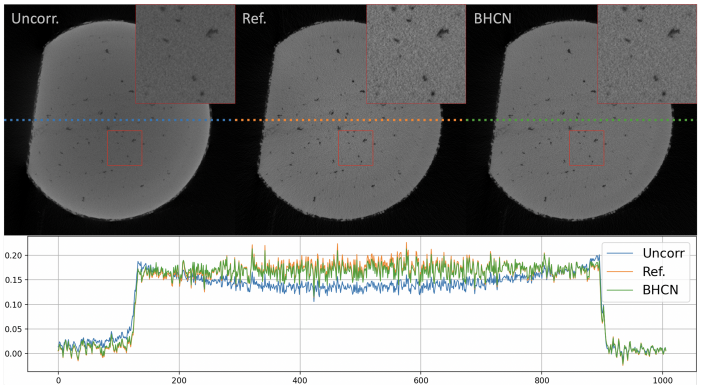

(a) AlCe

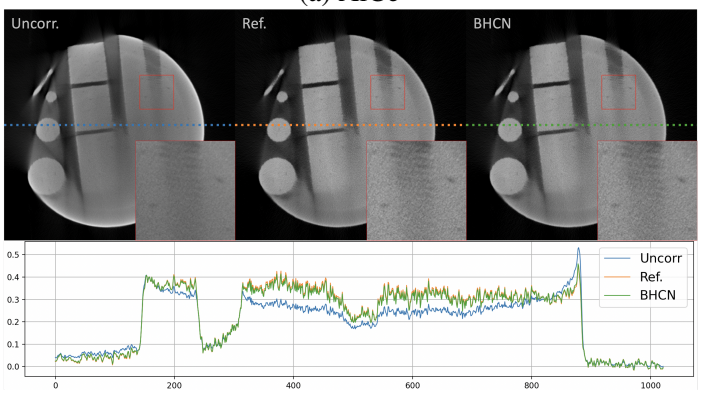

(b) NiCo

Figure 4: (left to right) No correction, reference, BHCN; Profile plot. BHCN reduces beam hardening artifact as much as the reference method as evident from the reduction in cupping artifact. Both reference and BHCN have better defect contrast in the RoI.

3.2.2 Robustness across various geometries

AM allows for printing of complex geometries, which in turn complicate beam hardening correction for XCT scans of those components. Despite that, our results suggest that the BHCN extends very well to complicated geometries. In Fig. 5 BHCN reduces BH in the top and bottom subfigures (pentagon and flower vase), and has more uniform-looking image than the reference subfigure (blade).

4 Conclusion

We developed a BHC network (BHCN) that is more robust than a baseline curve-fit method and compares well against the recently proposed CAD- and physics–based reference method that needs to be calibrated for each alloy. Our experiments show that the BHCN reduces BH for most alloys currently used in AM, and for different geometries. It also furnishes better defect contrast that should lead to more accurate defect characterization. Further, BHCN performs BHC by reducing cupping artifacts and producing uniform-looking images for all the alloys we tested for. We have also demonstrated that BHCN works well with simulation and real data despite the absence of accurate segmentation for the distance data needed for BHCN input. This supports the claim that in practical scenarios where perfect segmentation is not possible, BHCN can still perform beam-hardening reduction robustly without any retraining, calibration, or knowledge of the component material.

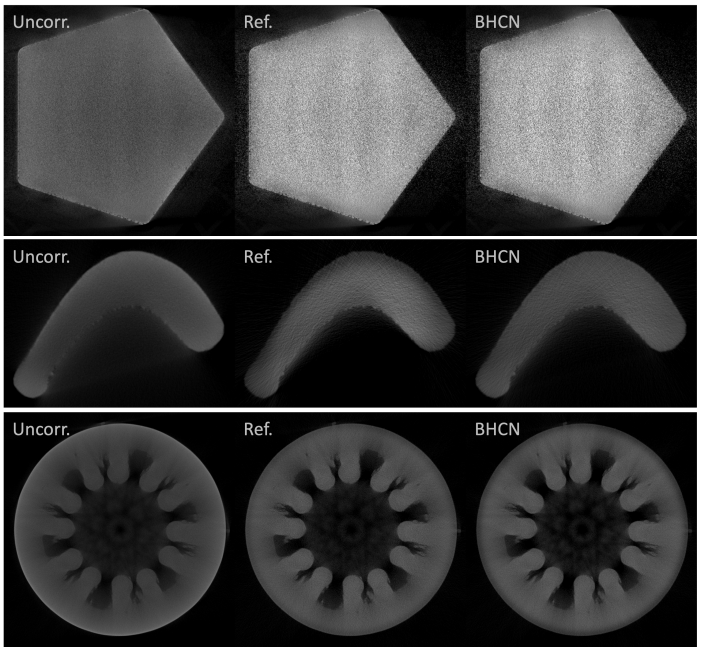

Figure 5: Different geometries and AM processes: (Top to bottom) Pentagon, blade and flower vase; (left to right) No correction, reference, BHCN. Both correction methods have similar reduction in BH for pentagon and vase, but BHCN blade metal part looks more uniform than that of the reference.

References

[1] M. Brennan, J. Keist, and T. Palmer. “Defects in metal additive manufacturing processes”. *Journal of Materials Engineering and Performance* 30.7 (2021), pp. 4808–4818.

[2] D. Svetlizky, M. Das, B. Zheng, et al. “Directed energy deposition (DED) additive manufacturing: Physical characteristics, defects, challenges and applications”. *Materials Today* 49 (2021), pp. 271–295.

[3] Q Yang, W. Fullagar, G. Myers, et al. “X-ray attenuation models to account for beam hardening in computed tomography”. *Applied Optics* 59.29 (2020), pp. 9126–9136.

[4] O. Rahman, K. D. Sauer, C. J. Evans, et al. “Direct Iterative Reconstruction of Multiple Basis Material Images in Photon-counting Spectral CT”. *The 6th International Conference on Image Formation in X-Ray Computed Tomography*. 1. 2020, pp. 462–465.

[5] G. T. Herman. “Correction for beam hardening in computed tomography”. *Physics in Medicine & Biology* 24.1 (1979), p. 81.

[6] P. Jin, C. A. Bouman, and K. D. Sauer. “A model-based image reconstruction algorithm with simultaneous beam hardening correction for X-ray CT”. *IEEE Transactions on Computational Imaging* 1.3 (2015), pp. 200–216.

[7] E. Van de Casteele, D. Van Dyck, J. Sijbers, et al. “An energy-based beam hardening model in tomography”. *Physics in Medicine & Biology* 47.23 (2002), p. 4181.

[8] L. A. Feldkamp, L. C. Davis, and J. W. Kress. “Practical cone-beam algorithm”. *Josa a* 1.6 (1984), pp. 612–619.

[9] N. Otsu. “A threshold selection method from gray-level histograms”. *IEEE transactions on systems, man, and cybernetics* 9.1 (1979), pp. 62–66.

[10] A. Ziabari, S. Venkatakrishnan, A. Lisovich, et al. *High Throughput Deep Learning-Based X-ray CT Characterization for Process Optimization in Metal Additive Manufacturing*. Tech. rep. 2022, pp. 160–164.

[11] A. Ziabari, V. Singanallur, Z. Snow, et al. “Enabling Rapid X-ray CT Characterisation for Additive Manufacturing Using CAD models and Deep Learning-based Reconstruction” (2022).